Exciton–plasma transition in nonuniformly deformed germanium

I. V. Kukushkin, V. D. Kulakovskiĭ, T. G. Tratas, and V. B. Timofeev

Institute of Solid State Physics, USSR Academy of Sciences
(Submitted 24 August 1982)
Zh. Eksp. Teor. Fiz. **84**, 1145–1157 (March 1983)

The photovoltaic properties of Ge crystals in a magnetic field crossed with the nonuniform strain field (photovoltaic-piezomagnetic (PVPM) effect) was investigated at high-excitation densities and at low temperatures. The dependences of the short-circuit current and of the transverse photo-emf on the pump, on the magnitude and direction of the strain, on the temperature, and on the magnetic field are investigated. An abrupt jump of the photocurrent is observed at sufficiently high pumping and can be attributed to an exciton–plasma transition in a system of drifting excitons. It is established that the photocurrent jump is accompanied by a threshold-dependent appearance of a new spectral line corresponding to radiative recombination of an e–h plasma. The exciton-density distribution is investigated in the direction of the drift towards the center of the deformation potential well and the causes of the onset and spatial localization of a plasma filament are analyzed. The experimentally obtained critical density for the exciton–plasma transition is found to be $n_c \approx 7\times 10^{15}$ cm^{-3} ($r_s^c \approx 2$) and agrees with the criterion for dielectric screening of the Coulomb interaction.

PACS numbers: 72.40. + w, 72.80.Cw, 71.35. + z, 75.80. + q

§1. INTRODUCTION

At high densities of the nonequilibrium electron-hole gas the excitons are collapsed by ionization because of the screening of the Coulomb interaction. At low temperatures ($kT \ll R$, where R is the exciton Rydberg) the transition of the excitons into an electron-hole plasma, in direct analogy with the insulator–metal transition, should, according to the Mott hypothesis,[1] proceed jumpwise when the exciton density reaches a critical value n_c (or, using dimensionless units $r_s = (4/3\pi n a_{ex}^3)^{-1/3}$, at the critical value r_s^c). It is natural to expect the ionization collapse of the excitons to be accompanied by a jumplike change of the electric transport properties. In the first experiments on Ge at 2 K, an attempt was made to make an exciton–plasma transition observable by the jump of the photoconductivity.[2] Later, however it became clear that the abrupt increase of the photoconductivity observed in Ge at high excitation density is due not to ionization collapse of the excitons, but to percolation conduction over the metallic electron-hole drops (EHD), into which the excitons condense.[3,4] In undeformed germanium crystals, the e-h liquid has a large binding energy, therefore at low temperatures condensation of excitons into EHD takes place at substantially lower densities than the critical density n_c (as a result, n_c turns out to be in the two-phase region at low temperatures).[4] In the high-temperature region (including the region $T > T_c$), the transition of excitons into an electron-hole plasma is greatly smeared out because of the thermal dissociation of the excitons, therefore the corresponding changes observed in the exciton recombination (absorption) spectra when n_c is approached have likewise a smeared out (diffuse) character.[4,5]

The most promising for the observation of exciton–plasma transition are uniaxially deformed Ge and Si crystals, in which, owing to the lifting of the degeneracy of the bands, the stability of the EHD and the critical condensation temperature decrease. Because of this, at sufficiently low temperatures, it is possible to realize in the crystals exciton-gas densities close to the critical value n_c.[6,7]

We reported in a short letter[8] observation of a giant jump of the short-circuit current in Ge crystals in a magnetic field crossed with the nonuniform strain field at large excitation densities; this was attributed to an insulator–metal transition in a system of drifting excitons of high density. The photovoltaic properties in crossed magnetic fields and the field of the inhomogeneous deformation (the so called photovoltaic-piezomagnetic (PVPM) effect) turned out to be an effective tool for the investigation of the exciton-plasma transition. Indeed, in the considered PVPM effect, the electrons and the holes, which are bound into excitons, begin to contribute to the short-circuit current only as a result of the ionization collapse of the excitons when the critical density is reached. With the aid of a special nonuniform compression geometry (see §2) it is possible to localize spatially the region of exciton-plasma transition. Because of this, it is possible to observe with the aid of the PVPM the change of the crystal conductivity, which reached more than three orders of magnitude at low temperatures. In the present article, in addition to the photovoltaic properties (see §3), we investigate the recombination-radiation spectra in the region of the exciton–plasma transition (§4). As a result we determine the critical density and establish the spatial localization of the exciton–plasma transition inside the crystal. Finally, in §5 is given in analysis of the distribution of the exciton density and the direction of the exciton drift under the experimental conditions.

§2. EXPERIMENTAL PROCEDURE

We investigated germanium single crystals with residual impurity densities 3×10^{12}–3×10^{11} cm^{-3}, which were cut in the form of rectangular parallelepipeds with linear dimensions $3\times 3\times 10$ mm. The samples were placed directly in liquid helium. To decrease the surface recombination prior

 0038-5646/83/030665-08$04.00

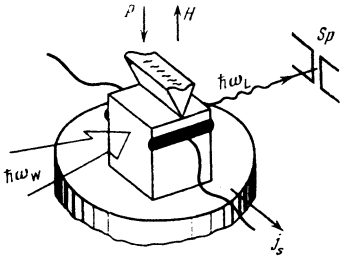

FIG. 1. Experimental setup.

to placing them in the cryostat, the crystals were etched in the polishing etchant CP-4a.

The nonequilibrium carriers were excited with a cw neodymium laser using an aluminum yttrium garnet (1.064 μm), with power up to 10 W. The spectral instrument was a double monochromator with gratings of 600 lines/mm and a dispersion in the working region 8 Å/mm. The radiation was recorded with a cooled Ge(Cu) photoresistor in the synchronous-detection regime. The modulation frequency of the 1.064 μm laser amounted in this case to 60 Hz. To record the differential spectra (with respect to excitation density) of the radiation, a semitransparent modulator of the laser radiation was used, with modulation depth $\approx$15–20%.

For the electric measurements, indium contacts in the form of strips were soldered to the lateral faces of the sample (Fig. 1). To improve the ohmic properties of the contacts, they were punched through with high-frequency discharge. After this, the contacts remained symmetrical down to helium temperatures, and their deviation from ohmic, as will be seen from the discussion of the results, was insignificant. The procedure for obtaining large uniaxial strains is analogous to that used by us earlier in Ref. 7. Nonuniform deformation of the crystals was produced with a triangular brass prism. In this case an axisymmetric strain potential well was produced in the interior of the crystal, at a depth of approximately 0.5 mm under the sharp edge of the prism.

The geometry of the experiment is shown in Fig. 1. In this geometry it is possible to measure simultaneously the short-circuit current and the transverse voltage in the PVPM effect, and also to record the spectra of the integrated radiation from the sample. In a number of cases, in the absence of ohmic contacts, the radiation was recorded in a direction parallel to the face of the prism. In this case it was possible to record the spectra from sections with different degrees of uniaxial strain. Information on the spatial localization of the processes that occur in the crystal could be obtained in a number of experiments by using pointlike ohmic pairs of contacts (*A* and *B* in Fig. 6 below). The magnetic field, in the investigation of both the PVPM and of the photovoltaic-magnetic (PVM) effects, was always directed along the crystal deformation axis ⟨100⟩ or ⟨111⟩.

§3. PHOTOVOLTAIC PROPERTIES UNDER CONDITIONS OF EXCITION-PLASMA TRANSITION

The photovoltaic-piezomagnetic effect, just as other galvanomagnetic effects, is based on the fact that the free carriers moving in an nonuniform-strain field in a direction perpendicular to the magnetic field **H** are deflected under the action of the Lorentz force in a direction perpendicular to **H** and to the gradient of the strain potential. The result is a transverse voltage $V_\perp$, and when the circuit is shorted, a corresponding current j_s. The idea of using this effect for the study of exciton-plasma transitions is simple–so long as the electron and the hole are bound into an exciton, they move under the influence of the force ∇E_g due to the inhomogeneous strain, experience practically no deflection in the magnetic field, and make no contribution to the short-circuit current. If, after a certain critical exciton density is reached, the excitons are collapsed by ionization, the current j_s should increase abruptly. Such a jumplike increase of j_s was observed by us in Ge crystals nonuniformly compressed along the axes ⟨111⟩ and approximately ⟨001⟩ in the compression geometry shown in Fig. 1, at temperatures $T = 2$–6 K.

Figure 2 illustrates the change of the dependences of the short-circuit current j_s and of the photo-emf $V_\perp$ on the pump W when the deformation **P** is increased along the ⟨111⟩ axis and at $T = 2$ K. At zero pressure (the situation of the usual photovoltaic-magnetic effect), j_s increases monotonically with increasing W. Starting with pressures $P \gtrsim 50$ MPa the function $j_s(W)$ undergoes a jump.[1)] The amplitude and slope of the photocurrent jump first increase with increasing strain, and at large P ($\gtrsim 300$ MPa) they cease to depend on the strain. The transverse photo-emf depends little on W at all strains and decreased somewhat only in the region of the photocurrent jump. At $P = 0$ the voltage $V_\perp$ is almost constant. We note that the experimentally observed values of the photo-emf are insufficient for impact ionization of the exci-

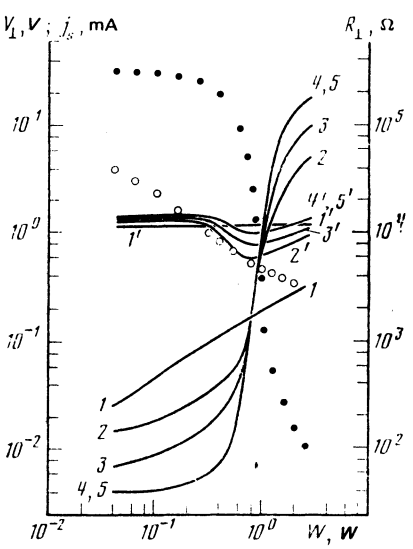

FIG. 2. Dependences of the short-circuit current j_s, of the transverse photo-emf $V_\perp$, and of the transverse magnetoresistance $R_\perp$ on the pump W and $T = 2$ K, $H = 0.7$ T, and different values of deformations directed along the ⟨111⟩ axis. Curves 1–5 corresponds to $j_s(W)$ dependences at respective deformations 0, 70, 150, 230, and 350 MPa. Curves 1′–5′ correspond to the $V_\perp(W)$ dependence at the same deformations. The $R_\perp(W)$ dependences measured at $P = 0$ and $P = 350$ MPa are shown by light and dark circles, respectively.

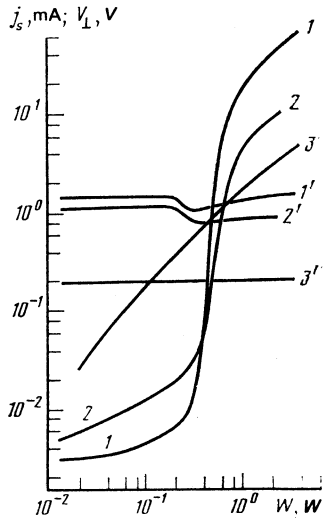

FIG. 3. Plots of $j_s(W)$ and $V_\perp(W)$, measured at a strain 420 MPa, directed along an axis close to ⟨100⟩, a magnetic field $H = 0.7$ T, and different temperatures: 2 K—curves 1 and 1'; 5 K—curves 2 and 2'; 20 K—curves 3 and 3'.

tons.[9] We note also that in the region of pumps prior to the jump of the photocurrent, at the produced $V_\perp$, the excitons continue to be distinctly observed in the recombination spectra (see §4).

Figure 3 shows the behavior of $j_s(W)$ and $V_\perp(W)$ at various temperatures. It can be seen that the jump in the $j_s(W)$ dependence exceeds three orders of magnitude at $T = 1.7$ K, amounts to two orders at $T = 4.2$ K, and vanishes completely at $T = 20$ K, when the excitons are strongly thermo-ionized. We recall that in Ge strongly compressed along the ⟨111⟩ axis the exciton Rydberg is $R = 2.65$ meV.[10]

As expected, when the direction of the magnetic field is changed the short-circuit and the photo-emf in the PVPM effect reverse sign (Fig. 4). The small difference in the behavior of $j_s(W)$ with change of direction of H is due to the nonohmic character of the contacts (to the influence of the contact potential difference) and, as seen from Fig. 4, is not substantial.

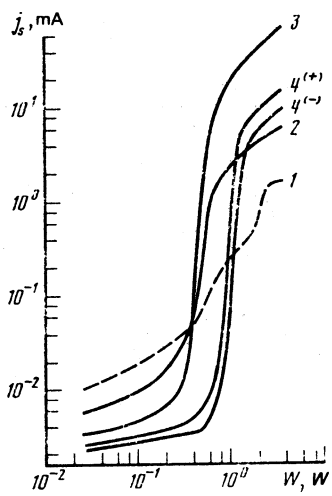

FIG. 4. Plots of $j_s(W)$, measured at $T = 2$ K, of the deformation 420 MPa applied along an axis close to ⟨100⟩, and at different values of the magnetic field: 0.05 T—curve 2; 0.7 T—curve 3; 3.2 T—curves $4^{(+)}$ and $4^{(-)}$. Curves $4^{(+)}$ and $4^{(-)}$ differ only in the direction of the magnetic field. Curve 1 was plotted at $H = 0$ in an electric field 1.5 V/cm.

The jumps of j_s observed in strongly compressed crystals Ge⟨001⟩ and Ge⟨111⟩ at large excitation density and at sufficiently low temperatures can be naturally explained as being due to ionization collapse of the excitons when the critical density is reached. With increasing temperature, the fraction of the thermally ionized excitons increases, j_s becomes smeared out and vanishes in final analysis at $T \gtrsim 20$ K. It is significant that the current jump is observed above the critical temperature for exciton condensation into EHD (in Ge⟨001⟩ at $P \gtrsim 300$ MPa the critical EHD temperature is $T_c \lesssim 4$ K, Ref. 7). At $T > T_c$ the jump of j_s takes place practically at the same excitation densities as at $T < T_c$ (one can compare curves 1 and 2 of Fig. 3). It can therefore be suggested that at $T < T_c$ the observed behavior of $j_s(W)$ is likewise due not to percolation over the metallic electron-hole drops, but to an exciton-plasma transition. This interpretation is confirmed by investigations of the behavior of the short-circuit current $j_s(W)$ when the magnetic field is varied (Fig. 4). In the region $H \lesssim 1$ T the threshold of the rapid increase of the photocurrent does not depend on the magnetic field, and the amplitude of the current jump increases with increasing H. When the magnetic field is increased, in the region $H \gtrsim 1.5$ T the photocurrent threshold is monotonically shifted towards higher excitation densities. This result correlates well with the decrease of the transverse dimension of the wave function of the exciton with increasing H in this region, and does not have a simple explanation within the framework of the model of percolation over the EHD. In addition, we note that in case of percolation of the current over the EHD there should be observed oscillations of the photocurrent threshold when the magnetic field is swept.[3] These oscillations are due to the change in the density and dimensions of the EHD when the Landau levels pass through the corresponding Fermi levels, and amount to several percent in the undeformed Ge.[3] In the considered PVPM effect, no such oscillations are observed, despite the high sensitivity of the method ($\Delta W/W < 0.0\%$), which is ensured by the very strong dependence of the current on the pump in the vicinity of the threshold: $j_s(W) \propto W^9$!.

Let us dwell on the question of the transverse magnetoresistance $R_\perp(H)$ of a plasma filament produced in the interior of the crystal as a result of the exciton–plasma transition. The corresponding plots of $j_s(H)$, $V_\perp(H)$, and $R_\perp(H)$ obtained in Ge⟨100⟩ at an excitation density slightly exceeding the threshold are shown in Fig. 5. It is seen directly from the figure that these plots show no oscillations whatever, and $R_\perp(H)$ is a quadratic function of the magnetic field. In the case of a two-component electron-hole plasma, in the limit of the strong magnetic field realized in our experiment, $R_\perp$ is given by the expression (see, e.g., Ref. 11):

$$R_\perp(H) = R_\perp(0)\,[1+(\Omega_c\tau_{eff})^2], \qquad (1)$$

where Ω_c is the cyclotron frequency and τ_{eff} is the effective time of carrier relaxation.

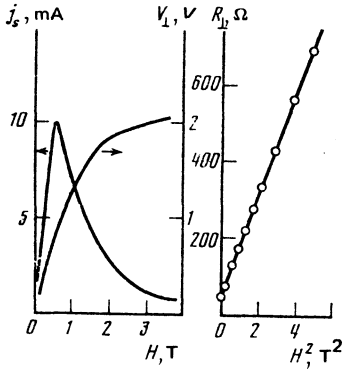

FIG. 5. Plots of $j_s(H)$, $V_\perp(H)$, and $R_\perp(H)$ at $T = 2$ K and at a deformation 420 MPa directed approximately along ⟨100⟩.

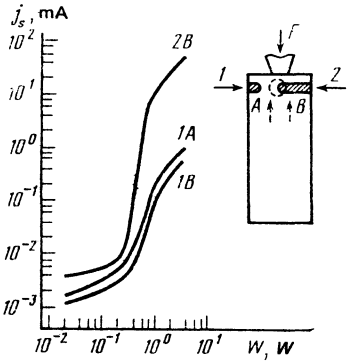

FIG. 6. Plots of $j_s(W)$ measured in the presence of pairs of contacts A and B shown in the inset of the figure. The arrows with the numbers show the direction of propagation of the exciting light. The hatches mark the region of the deformation potential well. $T = 2$ K, $H = 0.7$ T, and the deformation 310 MPa is directed along the ⟨100⟩ axis.

From the experimental plot of $R_\perp(H)$ in Fig. 5 we obtain for τ_{eff} the value $(1.2 \pm 0.1)\times 10^{-11}$ sec, which is smaller by an order of magnitude than the characteristic time of carrier scattering by phonons at the employed temperatures 2–4 K. In the investigated pure crystals of germanium it is likewise certainly possible to neglect scattering by impurities. The experimentally obtained value of τ_{eff} is close to the time of the electron-hole scattering in an e–h plasma, which can be estimated at $kT \ll E_F^{e,h}$ from the formula[12]

$$\tau_{eh} = \left(\frac{3}{4\pi\hbar}\right)^{1/3}\left[\frac{E_F^e E_F^h}{(kT)^2}\right]\left(\frac{m_{de}m_{dh}}{4E_F^e E_F^h}\right)^{1/4}, \qquad (2)$$

where $E_F^{e(h)}$ is the Fermi energy of the electrons (holes), and $m_{de}(m_{dh})$ is the mass of the density of states of the electrons (holes). It is known[11] that in the case of isotropic electron and hole dispersion laws the electron-hole scattering makes no contribution to the magnetoresistance. It is not excluded, however, that in germanium crystals this scattering is significant because of the strong anisotropy of the effective masses of the electrons. This question remains open so far.

We turn now to the question of where in the sample is the large short-circuit current generated. From the geometry of the experiment (Fig. 1) it can be seen that one can single out three characteristic regions: 1) the subsurface region, in which the nonequilibrium carriers are generated; 2) the region of maximum strain (or the bottom of the potential well) near the center of the crystal, to which the nonequilibrium e–h pairs flow off, and 3) the intermediate region, in which the nonequilibrium carriers, excitons, and EHD (at $T < T_c$) flow under the influence of the strain-potential gradient. From the viewpoint of the electric circuit, these three regions are connected in parallel. Starting from the nature of the galvanomagnetic effects, we can exclude from consideration the potential-well region, where the drift velocity of the e-h pairs is extremely small. Percolation over the EHD at the bottom of the potential well (at $T < T_c$) can lead only to shunting of the source of the photo-emf and to a decrease of $V_\perp$. This effect, however, is weak, since it can be seen from Fig. 2 that $V_\perp$ changes little in the region of the threshold increase of j_s.

To demarcate the intermediate and the subsurface regions, experiments were performed in which two pairs of individual contacts, A and B were used. One of them (A) was located directly near one surface of the crystal, and the other pair (B) started out from its opposite surface and ended in the region of the center of the potential well (Fig. 6). In the case of excitation of the crystal from the site of the contact B, a characteristic jump of the photocurrent was observed on the contacts B, with amplitudes of approximately three orders of magnitude (curve 2B). In the case of illumination from the side of the contact A, a jump of the photocurrent is observed both on the subsurface contacts (curve 1A) and on the contacts located in the region of the potential-well bottom (curve 1B), but its amplitude is weaker by one-and-a-half or two orders of magnitude (observation of the jumps in the two last cases is natural, if it is recognized that the volume of the sample has a finite resistance). It follows from this experiment that the large short-circuit current is produced not in the subsurface region and not in the region of the potential well, but in an intermediate region (the place where a conducting plasma filament is expected to occur is shown in Fig. 6 by dashed arrows). From the plots of $j_s(W)$ and $V_\perp(W)$ it follows that the conductivity of the crystal at the instant of the transition increases by four orders of magnitude.

Thus, on the basis of the results obtained in the investigation of the PVPM effect it becomes possible not only to establish that the jump of the short-circuit photocurrent is due to an exciton–plasma transition, but also roughly separate the crystal region where such a transition takes place under the realized nonuniform deformation. With the aid of electric measurements alone, however, it is impossible to determine the critical density of the excitons and to ascertain the causes of the strong $j_s(W)$ dependence under strong nonuniform deformation. The role of the electron-hole drops at $T < T_c$ also remains unexplained. We shall attempt to obtain answers to these questions by investigating the radiative recombination spectra.

§4. RADIATIVE RECOMBINATION SPECTRA UNDER CONDITIONS OF EXCITON–PLASMA TRANSITIONS

Figure 7 shows the emission spectra of inhomogeneously compressed Ge⟨001⟩ crystals, plotted at $T = 2$ K for excitation in the upper edge of the sample, in the geometry shown in Fig. 1. At low excitation densities $W \lesssim 1$ W/cm^2

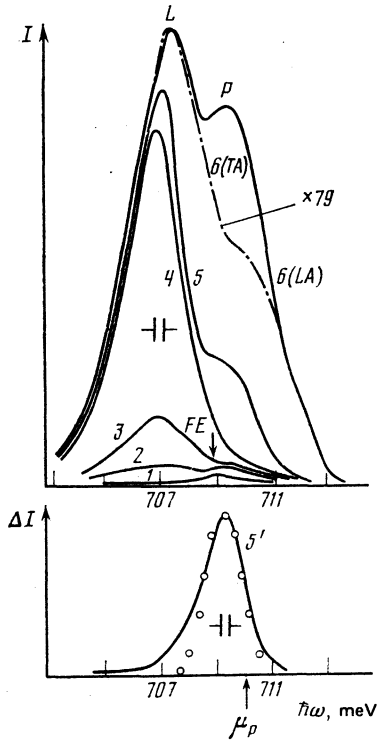

FIG. 7. Emission spectra of Ge⟨100⟩, measured at $T = 2$ K, $H = 0$ T, and $P = 420$ MPa at different values of the excitation density: *1*—1; *2*—2; *3*—10; *4*—65; *5*—80; *6*—180 W/cm^2. The spectra 1–6 correspond to the *LA* component of the spectrum, the spectrum 6(*TA*) is included in the *TA* component and is shifted towards lower energies, for convenience in comparison, by an amount equal to the difference between the energies of the *LA* and *TA* phonons. 5′—differential spectrum of the *LA* component 5. The circles show an approximation of the shape of the spectrum.

there appears in the spectrum one emission line, from the half-width and spectral position of which we can conclude that it is due to the emission by excitons moving in the potential well. The half-width of this line (≈ 1 meV) exceeds noticeably that expected for excitons in a potential well at equilibrium with the lattice (3 kT$\approx$0.5 MeV) and consequently the drift time of the electrons in the potential well turns out to be in our experiment comparable with their lifetime. The causes of the difference between the carrier drift velocities in our experiment and with the data of Ref. 13 will be discussed in detail in Ref. 14. With increasing pump (curve 2, Fig. 7) there appears in the spectrum also a line *L* of emission from EHD located at the bottom of the potential well. With further increase of the pump the intensity of this line in the spectrum increases (spectra 3 and 4) whereas the intensity of the exciton line *FE* remains practically unchanged.

At pumps corresponding to the threshold of the increase of the photocurrent in the PVPM effect, there appears in the emission spectra a new emission line *P*, the half-width of which is somewhat smaller than that of the line *L*, but noticeably larger than of the exciton line *FE*. This line *P* can be naturally attributed tor radiation of the *e–h* plasma produced as a result of ionization collapse of the excitons. The line *P* can be especially well separated in differential (with respect to power) excitation of the spectrum (Fig. 7, spectrum 5′ was plotted at 15% modulation of the pump power).

It was established that the magnetic field in the region $H \lesssim 1.5$ T not only does not influence the threshold of the growth of the short-circuit current, but does not change also the shape and the relative intensities of the lines *FE*, *L*, and *P* in the entire interval of the realized pumps. This means that in the indicated regions the magnetic field does not influence the partial composition of the *e–h* system and affects little the critical parameters of the exciton-plasma transition. We shall therefore seek the parameters of the *e–h* plasma with the aid of analysis of the recombination spectra measured in a zero magnetic field. In this case one can determine the density of the *e–h* plasma responsible for the appearance of the *P* line in the spectrum, by analyzing its shape with the aid of the expression[15]

$$I(h\nu) \propto \int_0^{h\nu} D_e(E) f_e(E) \times D_h(h\nu - E) f_h(h\nu - E)\, dE, \tag{3}$$

where $D_{e(h)}$ and $f_{e(h)}$ are the densities of states and the distribution functions of the electrons (holes). In expression (3), the density n is the only adjusting parameter. In the case of inhomogeneously compressed crystals, this expression can be used under the condition that the *e–h* plasma is localized in a narrow region Δx in the direction of the deformation-potential gradient, so that the change of the width of the forbidden gap in this interval, Δx, is much larger than the Fermi energies of the electrons and the holes or kT (in the nondegenerate case). It can be seen from Fig. 7 that at an excitation density near the threshold value ($W \approx 1.2 W_0$) expression (3) describes quite satisfactorily the shape of the line *P*, if the *e–h* plasma is assumed to be $n_P = 7 \times 10^{15}$ cm^{-3} ($r_s = 1.95$). When the excitation density is increased, the *P* line broadens somewhat and its shape is not as well described by expression (3). Thus, it can be suggested that at $W \approx W_0$ the exciton–plasma transition takes place in a very narrow region of Δx. With increasing W, this region broadens and it is not excluded that in this case the density of the *e–h* plasma increases somewhat. The estimate obtained above for the density n_P is the upper bound for n_c. It is therefore desirable to have an independent and more accurate method of estimating the density of the produced *e–h* plasma. In germanium crystals, the density of the *e–h* plasma can be determined from the ratio of the intensities (3) of the forbidden and allowed components of the radiation, corresponding to recombination of *e–h* pairs with emission of *TA* and *LA* phonons.[16] For a fixed band structure, the matrix elements of the transition for the recombination of the *e–h* pair with emission of a *TA* phonon M_{TA} is proportional to the wave vector k, while the emission of an *LA* phonon M_{LA} is independent of k. Therefore the ratio I_{TA}/I_{LA} is determined only by the density of the degenerate *e–h* plasma, namely, $I_{TA}/I_{LA} = A^* n^{2/3}$, where A^* is a constant that can be determined by analyzing the emission spectra of the EHD in uniformly compressed crystals. For Ge⟨100⟩ we have $A^* = 2.2 \times 10^{-13}$ cm^{-2}. From a comparison of the *TA* and *LA* spectra of the GE⟨100⟩ crystals at $W = 1.2 W_0$ (Fig. 7) we found that the density of the *e–h* pairs on the bottom of the potential well (the line *L*) amounts to $(1.4 \pm 0.1) \times 10^{16}$

cm^{-3}, while in a plasma filament responsible for the jump of the photocurrent (the line P) we have $n_P = (7 \pm 0.5) \times 10^{15}$ cm^{-3}. With further increase of the excitation density, despite the broadening of the P line, the ratio of the intensities of the TA and LA components for it remains unchanged within the limits of the 5% experimental error. It can thus be concluded that with increasing W above the threshold there takes place only a broadening of the region occupied by the e–h plasma, whereas its density changes very little. The agreement between the estimates $n_P = 7 \times 10^{15}$ cm^{-3} on the basis of the line shape at $W = 1.2W_0$ and obtain from the ratio of the intensities of the allowed and forbidden components confirms the assumption made above that near the threshold of the photocurrent the exciton-plasma transition takes place in a rather narrow region Δx, whose size can be estimated from the spectral broadening $\Delta h\nu$ of the P line and from the value of the gradient of the width of the forbidden band, ∇E_g, i.e., $\Delta x \approx \Delta h\nu / |\nabla E_g|$. At that maximum pump, $\Delta x \approx 0.1$ mm.

An analysis of the emission spectra makes it also possible to refine significantly the region of localization of the exciton–plasma transition in the volume of the crystal. It follows from Fig. 7 that the chemical potential of an e–h pl;asma μ_P, determined from the position and shape of the line P, lies higher in energy than the chemical potential of the e–h system on the bottom of the potential well. Consequently, the experimentally recorded metallization of the excitons takes place not only far from the excited surface, but also at a noticeable distance (≈ 0.5 mm, judging from the relief of the deformation well and from the position of μ_P) from the center of the potential well. This means that for strong pumping the distribution of the exciton flux density along the trajectory of the exciton drifts towards the center of the potential well turns out to be a nonmonotonic function with a pronounced maximum. It is precisely in the region of the maximum of the distribution of the exciton density where an exciton-plasma transition takes place in final analysis. The nonmonotonic distribution of the exciton density along the force lines of the deformation field can occur only in the case when the exciton is acted upon not only by the strain force but also by an opposing force directed from the center of the potential well. Such a force, which increases the "viscous friction" of the excitons when the center of the well is approached, can be produced by the phonon wind caused by emission of long-wave phonons as a result of recombination of e–h pairs in the center of the potential well.[17] This question will be analyzed in the next section.

§5. DISTRIBUTION OF THE EXCITON DENSITY IN THE DIRECTION OF THE DRIFT TOWARDS THE CENTER OF THE POTENTIAL WELL

We shall assume that all the carriers generated on the surface produce a nonequilibrium (in the gas–liquid system) flux of excitons directed towards the bottom of the potential well. We assume that the exciton distribution $n(x)$ over the crystal thickness is due to motion of the excitons in the field of the nonuniform deformations towards the bottom of the potential well ($x = 0$) and to the interaction with the phonon wind that is produced by the electron-hole liquid which occupies the bottom of the well and is directed opposite to the exciton stream. To find $n(x)$ it is necessary to solve the continuity equation, which takes in the stationary case the form

$$\operatorname{div} \mathbf{S}(x) + n(x)/\tau_{ex} = 0. \tag{4}$$

The exciton flux density can be written in the form

$$\mathbf{S}(x) = -D\frac{dn}{dx}\mathbf{i} + \frac{D}{kT}\left(\frac{B}{x} - A\right)n(x)\mathbf{i}, \tag{5}$$

where $\mathbf{i}$ is a vector located in a plane perpendicular to the pressure axis and directed from the bottom of the potential well to some considered point of the excited spot. Under the experimental conditions, when the linear dimensions of the excitation spot ($l, d \approx 2$ mm) exceed noticeably the exciton diffusion length $l_D \approx 0.5$ mm, we can neglect the diffusion in a direction perpendicular to the drift, and assume the exciton motion to be one-dimensional. To simplify the calculation we assume that the force $A = dE_g/dx$ due to the deformation does not depend on the coordinate x. The phonon-dragging force B/x decreases with the distance from the axis of the cylinder occupied by the EHL, as does also the density of the phonon flux from this region. For the considered cylindrical symmetry of the system we can represent the quantity B, following Ref. 17, in the form $B = R_d^2 kT/R_0^2$ where R_d is the radius of the drop cylinder, and the parameter R_0 characterizes the force of dragging of the excitons by the phonons.

The boundary condition on the surface of the crystal ($x = a$) and on the boundary of the drop in the potential well ($x = R_d$) take respectively the form $S(a) = -J$ and $n(R_d) = n_T$, where J is the flux of the excitons on the crystal boundary, and n_T is the thermal-equilibrium density of the excitons in the gas phase. The radius of the drop cylinder can be obtained from the condition that the rates of creation of e–h pairs on the surface is equal to the rate of their recombination in the drifting exciton flux and in the drop:

$$Jld = \frac{n_0 \pi R_d^2 l}{\tau_d} + \int_{R_d} \frac{n(x)\,dx}{\tau_{ex}} ld, \tag{6}$$

where τ_d is the lifetime of the e–h pairs in the drop and l is the length of the drop cylinder.

Figure 8a shows the computer-calculated change of the exciton density $n(x)$ with increasing excitation power at the experimentally realized gradients $A = dE_g/dx \approx 7$ meV/mm and at different values of the parameter R_0. The change of the radius of the drop cylinder R_d, of the position in magnitude of the maximum $n(x)$ with increasing J at different values of dE_g/dx is illustrated by Fig. 8b. The main results of the calculations can be summarized as follows.

1. The nonmonotonic distribution of the exciton density $n(x)$ with a pronounced maximum occurs only in the presence of phonon wind from the region of the potential well occupied by the EHD. To reconcile the calculation with experiment it is necessary to assume a parameter R_0 that characterizes the force of the phonon dragging of the excitons, of the order of 10^{-2} cm. This does not contradict the lower-

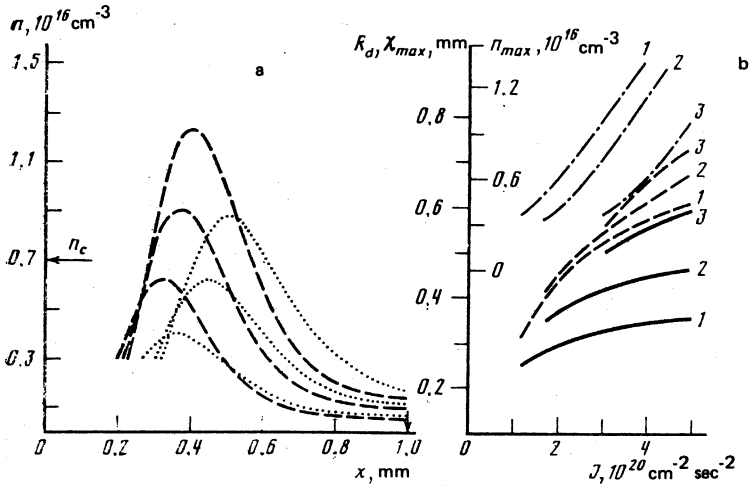

FIG. 8. a) Distribution of the exciton density $n(x)$ from the surface of the electron-hole drop to the surface of the crystal (shown by an arrow on the abscissa axis) at different e–h pair flux densities $J = (1.5,2,3)\times 10^{20}$ cm^{-2} sec^{-1} and at different values of R_0 characterizing the force of dragging of the excitons by the phonons: $R_0 = 7\times 10^{-3}$ cm (dashed curves) and $R_0 = 9\times 10^{-3}$ cm (dotted curves). The arrow n_c shows the experimental value of the density at which an exciton-plasma transition takes place. b) Calculated dependences of the position of the maximum of the exciton density x_{max} (dashed curves), of the exciton density n_{max} at the maximum of the distribution (dash-dot curves) and of the radius of the drop cylinder R_d (solid curves) on the flux density of the electron-hole pairs J at $R_0 = 9\times 10^{-3}$ cm and at different gradients of the deformation potential: 1) $A = 7$, 2) 11, 3) 16 MeV/mm. The calculations were performed for $n_0 = 1.5\times 10^{16}$ cm^{-3}, $d = 0.75$ mm, $\tau_d = 3\times 10^{-6}$ sec, $\tau_{ex} = 10^{-6}$ sec, and $T = 3$ K.

bound estimate for $R_0 \approx 5\times 10^{-2}$ cm, which can be obtained by following the calculations of Ref. 17.

2. With increasing pump, stabilization takes place of the radius of the drop cylinder: an increase of W by several times leads to a change in the volume of the drop only by tens of percent, which agrees qualitatively with experiment.

3. The density n_{max} first increases faster than linearly, and then linearly with increasing W. As noted above, no substantial increase of n_{max} was observed in experiment at $n > n_c$.

This result, however, can be understood if it is recognized that when the excitons collapse a change takes place also in the force of the phonon dragging of the e–h pairs.

It must be emphasized that the magnetic field, in the presence of which almost all the experimental results were obtained, is not a necessary condition for an exciton–plasma transition, inasmuch as already noted above, the emission spectra of the nonequilibrium e–h system in weak magnetic fields $H < 0.5$ T do not differ not only qualitatively but also quantitatively from the spectra at $H = 0$. This raises naturally the question of observing the crystal-conductivity change connected with the exciton-plasma transition in a zero magnetic field. Curve 1 of Fig. 4 illustrates the change of the photocurrent through the sample in the case $H = 0$ when an external source with emf 0.5 V is turned on ($E = 1.5$ V/cm). It can be seen that at the instant of the jump of the photocurrent in the PVPM effect the change of the photoconductivity in a zero magnetic field is small, but the plots of $j(W)$ still show a kink. Such a weak change of $j(W)$ at $H = 0$ compared with the giant increase of the short-circuit current in the PVPM effect is apparently due to two causes. First, owing to the selectivity of the PVPM effect, the shunting of the region of the exciton–plasma transition by a low-resistance region of the potential well turns out to be inessential. Second, the magnetic field improves considerably the homogeneity of the e–h system, causing motion of free electrons and holes perpendicular to the gradient of the deformation potential, as a result of which the electrons and holes are supplied from regions with high density, where the excitons have already become ionized ($n > n_c$) to neighboring regions where $n < n_c$.

§6. CONCLUSION

Thus, using Ge crystals as an example, we have shown the photovoltaic-piezomagnetic effect to be a precise tool for the investigation of the exciton–plasma transition. It became possible with its aid, for the first time ever, to observe a giant change in the electron transport properties in the case of ionization collapse of excitons. Analysis of the spectra of the radiative recombination measured under conditions of the jump in the photocurrent has made it possible not only to estimate the critical density of the exciton-plasma transition n_c, but also to establish spatial localization of this transition. Under the experimental conditions, in the case of strong inhomogeneous deformation, which produces in the crystal volume a potential well with axial symmetry, the region of the exciton–plasma transition turns out to be substantially localized in the direction of the exciton drift. The narrowness of the plasma filament produced in the transition and the homogeneity of the electron–hole density within its limits determine the sharpness of the photocurrent jump. These are the major advantages of the PVPM effect in the study of exciton–plasma transition compared with the usual procedure of measuring the photoconductivity in direct current at $H = 0$.

In the literature are discussed two criteria for the estimate of the critical density of the exciton–density transi-

tion.[10] According to Mott's criterion, where the approximation of plasma screening of the Coulomb interaction is used,[1] the critical density for a strongly deformed Ge⟨001⟩ crystal at $T = 2$ K should amount to $r_s^c \approx 4.5$. Within the framework of the second approach, the value of the critical density is estimated from the collapse of the energy gap in the spectrum of the single-particle excitations of the exciton system of high density. According to this approach, the excitons are destroyed by ionization at $r_s^c \approx 1.8$ (Ref. 18). The critical density of the exciton–plasma transition obtained by us and corresponding to $r_s^c = (2 \mp 0.1)$ comes close to the estimate calculated in the approximation of the dielectric screening of the excitons.[18] Less investigated and less understood are the kinetic properties of the carriers in the vicinity of the exciton-plasma transition. In this region, the motion of the carriers correlates strongly with the Coulomb interaction, which is not screened completely (electron–hole scattering). The mobility and the resultant conductivity of the carriers in this transition electron–plasma region is noticeably modified by *e–h* correlations. An investigation of this problem with the aid of the PVPM effect can be of independent interest.

The authors are deeply grateful to S. V. Iordanskiĭ and L. V. Keldysh for exceedingly helpful discussions, which stimulated the undertaking of certain experiments, and also to I. B. Levinson for a discussion of the influence of electron–hole scattering on the magnetoresistance.

[1)]The cited values of P were estimated from the spectral position of the emission line of the excitons from the deformation potential well and correspond to the pressure at its center.

[1]N. F. Mott, Adv. Phys. **16**, 49 (1967); Metal-Insulator Transitions, Barnes & Noble, 1974.
[2]V. M. Asnin and A. A. Rogachev, Pis'ma Zh. Eksp. Teor. Fiz. **7**, 464 (1968) [JETP Lett. **7**, 360 (1968)].
[3]V. F. Gantmakher and V. N. Zverev, Zh. Eksp. Teor. Fiz. **73**, 2337 (1977) [Sov. Phys. JETP **46**, 1223 (1977)].
[4]J. C. Hensel, T. G. Phillips, and G. A.Thomas, Sol. St. Phys. **32**, 87 (1977).
[5]Ya. E. Pokrovskii, and V. B. Timofeev, Sov. Sci. Rev. A, Vol. 1, 191, 1979.
[6]V. D. Kulakovskiĭ, I. V. Kukushkin, and V. B. Timofeev, Zh. Eksp. Teor. Fiz. **78**, 381 (1980) [Sov. Phys. JETP **51**, 191 (1980)].
[7]I. V. Kukushkin and V. D. Kulakovskiĭ, Zh. Eksp. Teor. Fiz. **82**, 900 (1982) [Sov. Phys. JETP **55**, 528 (1982)].
[8]I. V. Kukushkin, V. D. Kulakovskii, and V. B. Timofeev, Pis'ma Zh. Eksp. Teor. Fiz. **35**, 367 (1982) [JETP Lett. **35**, 451 (1982)].
[9]I. V. Kukushkin, V. D. Kulakovskiĭ, and V. B. Timofeev, Pis'ma Zh. Eksp. Teor. Fiz. **32**, 304 (1980) [JETP Lett. **32**, 280 (1980)].
[10]T. M. Rice, Sol. St. Phys. **32**, 1 (1977).
[11]V. F. Gantmakher and I. B. Levinson, Zh. Eksp. Teor. Fiz. **74**, 261 (1978) [Sov. Phys. JETP **47**, 133 (1978)].
[12]A. Monoliu and C. Kittel, Sol. St. Commun. **21**, 635 (1977).
[13]R. S. Markiewicz, J. P. Wolfe, and C. D. Jeffries, Phys. Rev. B **15**, 1988 (1977).
[14]I. V. Kukushkin and V. D. Kulakovskiĭ, Fiz. Tverd. Tela (Leningrad) **25**, (1983) [Sov. Phys. Solid State **25**, (1983)].
[15]Ya. E. Pokrovskii, Phys. Stat. Sol. (a) 11, 385 (1972).
[16]C. Benoit a la Guillaume, M. Voos, and F. Salvan, Phys. Rev. B **5**, 3079 (1972).
[17]V. S. Bagaev, L. V. Keldysh, N. N. Sibeldin, and V. A. Tsvetkov, Zh. Eksp. Teor. Fiz. **70**, 702 (1976) [Sov. Phys. JETP **43**, 362 (1976)].
[18]V. E. Bisti and A. P. Silin, Fiz. Tverd. Tela (Leningrad) **20**, 185 (1978) [Sov. Phys. Solid State **20**, 1068 (1978)].

Translated by J. G. Adashko